Biocompatible Surfaces for Specific Tethering of Individual Protein Molecules

Colin D. Heyes,[#,†] Andrei Yu. Kobitski,[#,†] Elza V. Amirgoulova,[#,†] and G. Ulrich Nienhaus*[,†,‡]

Department of Biophysics, University of Ulm, Albert Einstein Allee 11, 89069 Ulm, Germany and Department of Physics, University of Illinois Urbana-Champaign, Urbana, Illinois 61801

Received: March 2, 2004; In Final Form: June 16, 2004

We have characterized the biocompatibility of glass surfaces that were modified by protein layers or linear poly(ethylene glycol) (PEG) brushes with the aim of determining the optimal treatment for the immobilization of single biomolecules by specific attachment, which was done here using a streptavidin−biotin linkage. We have investigated the surface homogeneity by atomic force microscopy and the resistance to nonspecific binding by single-molecule detection of fluorescently labeled RNase H in a scanning confocal fluorescence microscope. The resistance to nonspecific binding of the surfaces was simply examined by omitting the biotin-streptavidin linkage in the surface preparation. We have also carried out fluorescence resonance energy transfer experiments to examine the ability of the surfaces to preserve the native state of specifically attached proteins via streptavidin−biotin linkage. Chemisorption and crosslinking of BSA or streptavidin to amino-functionalized glass yields excellent surface homogeneity and reproducibility, much better than physisorption onto bare glass. PEG 5000 films form the smoothest films and are very resistant to nonspecific protein adsorption, but PEG 2000 has significantly worse properties. Unlike protein-coated surfaces, PEG 5000 surfaces cause partial denaturation of the RNase H molecules, which we explain by intermingling of the PEG and polypeptide chains or by interaction of the underlying aminosilane layer with the protein. These results highlight the importance of a thorough surface characterization and design in fluorescence studies of immobilized single biomolecules.

Introduction

In recent years, single-molecule fluorescence microscopy has become very popular for the investigation of biological processes at the molecular level. Examination of individual biomolecules allows one to observe static heterogeneity and dynamic processes that are averaged out in ensemble (bulk) measurements. Examples include investigations of heterogeneous folding pathways,[1−3] conformational fluctuations of single proteins and nucleic acids,[4] flickering processes of fluorescent proteins[5,6] and heterogeneity in enzyme−substrate interactions.[7,8] Fluorescence correlation spectroscopy (FCS) on biomolecular solutions is a powerful technique with single-molecule sensitivity;[9] it allows one to study the dynamics of labeled molecules that diffuse through a small confocal volume (typically 1 fL) by analysis of the fluorescence autocorrelation function.[1,10−12] For solution FCS, sample preparation is fairly simple, which renders the method particularly useful for biomedical applications, for example in high-throughput screening.[13] However, solution FCS is not strictly a single-molecule technique, since a large number of molecules transiting the confocal volume contribute to the autocorrelation function. Moreover, molecules can only be studied during their brief sojourns within the confocal volume, which is determined by diffusion to ∼1 ms in aqueous buffer. Slower dynamics therefore escape detection. This problem can be circumvented by specific immobilization of biomolecules on surfaces.[4,5,8,14,15] Then, the observation time is only limited by the inevitable photobleaching of the fluorophores and not by diffusion. To be able to optically resolve individual molecules in the far field, they must be separated further than the extension of the point spread function (PSF) of the emitted light. Such a sparse coverage requires that the surfaces must be *extremely* inert toward nonspecific adsorption. Moreover, they should provide homogeneous environments that exert only minimal influence on the intrinsic biomolecular properties. Proteins are delicate, marginally stable systems. Unless we use well-engineered, biocompatible surfaces in these studies, we may not observe intrinsic properties of the proteins; rather, we may observe the effects of protein-surface interactions instead.

Minimally interacting surfaces exhibit, in general, hydrophilicity and electrical neutrality.[16,17] Extensive studies have been carried out on the molecular characteristics of biocompatible, self-assembled monolayers (SAMs).[16−19] Poly(ethylene glycol) (PEG) layers have been widely recognized as being extremely resistant to adsorption of many proteins.[20] Chain lengths and grafting densities were recognized as important parameters governing the inertness of PEG-derivatized surfaces to protein adsorption.[21−24] Traditional views have focused on steric repulsion as the key mechanism responsible for resistance toward protein adsorption, so that direct interactions between the bare surface and proteins are prevented.[22,25] More recently, Grunze and co-workers have emphasized the crucial role of interfacial water adsorption. Water was observed to penetrate into and bind to PEG SAMs, causing them to form amorphous layers with high water content.[26] Water adsorption depends strongly on the conformation of the PEG chains.[27,28] Thus, both detailed interactions at the molecular level and steric control have to be considered to fully understand protein adsorption resistance. Besides PEG−based surfaces, many other approaches have been used to engineer biocompatible surfaces, including

* To whom correspondence should be addressed: Tel: +49−731−5023051; Fax: +49−731−5023059; E-mail: uli@uiuc.edu.
† University of Ulm.
‡ University of Illinois Urbana-Champaign.
# These authors contributed equally to the work.

10.1021/jp049057o CCC: $27.50
Published on Web 08/06/2004

immobilization of vesicles,[2,15] lipid bilayers,[29−31] adsorbed proteins such as BSA,[4,32] Dextran[33] and Dextran-PEG copolymers,[34] and alkanethiolates.[35]

A variety of biocompatible surfaces has been employed in experiments with individual, immobilized biomolecules. Biotinylated lipid bilayer surfaces were used in DNA hybridization studies.[31] Staphylococcal nuclease enzymatic cleavage was investigated on surfaces derivatized with N-[(3-trimethoxysilyl)-propyl] ethylenediamine triacetic acid, which allows attachment of proteins with an engineered hexahistidine tag.[8] Physisorption of biotinylated bovine serum albumin (BSA) on hydrophilic glass surfaces has also been widely used to attach proteins via a (strept)avidin−biotin linkage.[4,32,36,37] This allowed conformational changes of an immobilized RNA 3-helix junction to be studied with varying Mg^{2+} ion concentration.[4] DNA hybridization measurements have also been performed on BSA-coated glass surfaces.[37] Other studies[32,36] followed the lateral movement of myosin molecules along an actin filament immobilized on the BSA-coated surface. In all applications, these BSA-derivatized surfaces retained the biological function of the molecules of interest. Typically, surface-immobilized biomolecules exhibit heterogeneous behavior, for instance in enzymatic turnover rates, but it is not yet clear how much of this 'molecular individualism' is a truly intrinsic property of the molecule. Interactions with a heterogeneous environment provided by the surfaces could also explain heterogeneity in functional assays.

The ideal surface for the immobilization of biomolecules should be homogeneously covered by the biocompatible material and interact with the biomolecule only through the tether by which the biomolecule is bound. Consequently, nonspecific adsorption will be negligible. For applications in protein folding, we also require that the surface is stable in a wide variety of solvents. For example, it should withstand denaturing chemical conditions, such as high concentrations of acid, urea, or guanidinium chloride (GdmCl). Using atomic force microscopy (AFM) and single-molecule fluorescence microscopy, we have systematically studied different surface coatings for immobilization of proteins with respect to three essential properties: (1) homogeneity of the layers, (2) resistance to nonspecific protein adsorption, and (3) ability to preserve the native fold of the specifically bound proteins.

Experimental Section

Growth and Labeling of RNAse H. The plasmid pJAL135C containing the gene for RNase H was supplied as a generous gift of Dr. S. Kanaya (Osaka University, Japan). In this plasmid, the three cysteine residues in the native sequence are replaced by alanines, and the glutamic acid at position 135 is substituted by a cysteine. The protein was overexpressed in *Escherichia coli* HB101 and purified as described previously,[38,39] with slight modifications. The purity of the protein was confirmed by SDS-gel electrophoresis and MALDI-TOF mass spectrometry. The protein was subsequently labeled at the primary amines of lysine residues with Alexa Fluor 546-NHS (Molecular Probes) and biotin-NHS (Sigma-Aldrich) according to the procedures recommended by the manufacturers. Dye labeling efficiency was determined by UV−vis absorption spectroscopy to be >70%.

For FRET measurements, a second cysteine was introduced for lysine 3 in the plasmid by site-directed mutagenesis using the Quikchange mutagenesis kit (Stratagene Europe, Amsterdam). The DNA primers for this procedure were synthesized by MWG-Biotech GmbH (Ebersberg, Germany). Standard cysteine-maleimide coupling was used with Alexa Fluor 546 maleimide and Alexa Fluor 647 maleimide (Molecular Probes) in a molar ratio 1:1:3 (protein:Alexa546:Alexa647) for more than 12 h at 4 °C in 20 mM phosphate buffer (pH 7.0). The protein molecules labeled with both a green and a red dye molecule were separated on a cation exchange column (RESOURCE S, Äkta-System, Amersham Pharmacia, Little Chalfont, United Kingdom) using a linear gradient of 0 to 1 M NaCl in 20 mM sodium phosphate buffer (pH 7.0), similar to the procedure described by Schuler et al.[1] Finally, the protein was biotinylated with biotin-NHS (Sigma Aldrich), as recommended by the manufacturer. All RNase preparations were stored and used in buffer A (20 mM Tris-HCl, 100 mM KCl, 10 mM $MgCl_2$, pH 7.4). Glycerol was added for long-term freezer storage.

Cleaning and Aminosilylation of Glass Coverslips. Untreated glass coverslips (24 × 32 mm^2 and 20 × 20 mm^2, Menzel, Braunschweig, Germany) were cleaned by brief combustion of contaminants in a flame followed by rinsing in buffer.[4] This has been shown to be a quick and effective method for the removal of fluorescent surface contaminants. To functionalize the coverslip surfaces with amino groups, they were first cleaned by O_2/Ozone plasma exposure for 10 min, followed by exposure to an ultrapure acetone (Selectipure grade, Merck) solution of a commercial aminosilane, Vectabond (Vector Laboratories, Burlingame, CA), according to the manufacturer's protocol. We found that silanization with this commercial aminosilane was more reproducible than by silanization with pure aminopropyl silane. Moreover, it did not necessitate the use of a glovebox. After 5 min exposure, the solution was removed by several washings of 18 MΩ Millipore water. Afterward, the surfaces were dried under a nitrogen flow. All silanization procedures were performed in a cleanroom to avoid contamination.

Biofunctionalization. For the adsorption of the biocompatible layer (BSA, streptavidin, PEG 2000, PEG 5000) onto the surface, a small channel was made as previously described.[4] For physisorption of protein molecules onto cleaned, nonfunctionalized glass substrates, biotin-labeled BSA or streptavidin (both from Sigma) was dissolved in phosphate buffer (pH 7.3) at a concentration of 1 mg/mL. The channel was filled so that the solution would adsorb to the surface for 10 min. Alternatively, for chemical bonding to the aminosilanized surface, standard EDC (Fluka Chemicals, Buchs SG, Switzerland) coupling was used.[40] This enabled the amino-functionalized surface to bind to the activated carboxylic acid groups of the protein. Moreover, the layer of immobilized proteins becomes crosslinked, as amino groups of the proteins can also react with neighboring carboxylic acid groups. Unbound protein was then rinsed out of the channel with Tris buffer solution. The buffer was left in the channel for another 15 min to quench any remaining activated carboxylic groups. Linear PEG chains were bound to the amino-functionalized surface using a 100 mg/mL (10% w/v) solution of mPEG-SPA MW 5000 or mPEG-SPA MW 2000 (Nektar Therapeutics, Huntsville, AL) in a 50-mM sodium carbonate buffer, pH 8.2. These PEG chains carried a succinimidyl function on one end that reacts with the amino groups on the silanized glass surfaces. To obtain a sparse coverage with specific binding sites for biotinylated proteins, Biotin-PEG-NHS MW 3400 (Nektar Therapeutics) was added to the PEG solution in a 1% weight ratio to nonbiotinylated PEG. The coverslip sandwich was then exposed to the PEG solution for 2 h, after which excess PEG was washed out with 18.2 MΩ Millipore water.

Single-molecule Fluorescence Microscopy. For specific binding of proteins to the BSA- or PEG-covered surfaces, a 10

μg/mL solution of streptavidin was exposed to the channel for binding to the exposed biotin groups on the surfaces. Then, the channel was exposed for 10 min to RNase H in buffer A, labeled with biotin and Alexa546 dye, to bind the protein to the surface via the already bound streptavidin. Subsequently, unbound RNase H was flushed out of the channel with buffer A. To examine nonspecific binding of RNase H to the surface, the channel was exposed for 10 min to the identical RNase H solution in buffer A, but by excluding the streptavidin linker protein. This is not possible for the streptavidin surfaces, so we used an identical concentration of RNase H in buffer A, labeled with the dye but not with the biotin. We verified that biotinylation of RNase H itself does not alter the adsorption properties of RNase H by comparing biotinylated and nonbiotinylated RNase H for nonspecific adsorption on biotinylated BSA and PEG surfaces. No difference was observed (results not shown).

Nonspecific and specific binding were assessed by analyzing the density of labeled molecules on the surfaces using a scanning fluorescence microscope of our own design, based on a Zeiss Axiovert 135 inverted microscope with Ar^+/Kr^+-ion laser (modified model 164, Spectra-Physics, Mountain View, CA) excitation. The laser beam was reflected by a dichroic mirror (532/633DCXR, AHF, Tübingen, Germany) and focused to a diffraction-limited spot in the sample by means of a water-immersion objective (C-Apochromat 63×/1.2W, Zeiss, Göttingen, Germany). A piezoelectric scanning stage (model P-731.20, Physik Instrumente, Waldbronn, Germany) allowed the sample to be scanned. The emitted fluorescence photons were collected by the same objective, passed through the dichroic mirror mentioned above, and focused onto a confocal pinhole (to reject photons emitted outside of the focal plane). A second dichroic mirror (650DCXRU, AHF) splits the beam into a green channel and a red channel, which are further filtered with an HQ582/50 filter (AHF), and an HQ665LP filter (AHF), respectively. Photons in each channel were independently detected using avalanche photodiodes (SPCM-AQR-14, Perkin-Elmer, Vaudreuil, Canada). Their output signals were registered in a control card interfaced to a PC. Homemade software controlled the stage scanning (integration time 5 ms/pixel) and image acquisition. Typically, images of 18 μm × 18 μm^2 regions were collected at a resolution of 128 × 128 pixels.

Atomic Force Microscopy Measurements. For the AFM measurements, the surfaces were prepared in the same way as for fluorescence microscopy, except that the top coverslip was omitted to allow the AFM tip access to the surface. AFM images were obtained with a NanoScope IIIa (Digital Instruments, Mannheim, Germany). Tapping mode cantilevers (Olympus Optical Corporation, Hamburg, Germany) with spring constants of ~42 N/m were used for the imaging at a frequency of ~300 kHz in air with a scan rate of 2 kHz.

Results and Discussion

Like BSA, most protein molecules will readily adsorb to bare glass surfaces. This is a major problem in the biomedical field, where it is often required that surfaces resist protein adsorption (e.g., from blood). Preadsorbing BSA onto the surface allows one to limit nonspecific adsorption of other biomolecules of interest, which can subsequently be attached specifically by using (strept)avidin−biotin.[4,32,36,37] In single-molecule functional assays, researchers have so far paid little attention to ensuring minimal protein-surface interactions so that the results are characteristic of the immobilized protein and not affected by a particular surface preparation. It has, however, been recognized from bulk studies that these protein interactions with coated glass surfaces depend sensitively on the protein, the surface, and the solution conditions.[35,41] For example, the interaction potential experienced by a protein in proximity to a biocompatible coated surface depends highly on the distance from the surface and on the coating.[22,25] Thus, heterogeneities in surface thickness and structure will affect the details of the energy landscape of the protein. We have performed a systematic study of surface structure and biocompatibility using two proteins, BSA and streptavidin, as examples. We have adsorbed them physically as well as chemically (via peptide bonds) on glass surfaces. We compare these adsorbed proteins to PEG (MW 2000 or 5000), which has been chemisorbed to the glass. Schematics of these adsorptions are summarized in Figure 1. We expect that functionalizing the glass with reactive amine groups prior to protein exposure will lead to a more homogeneous coverage than adsorption onto bare glass, as well as being more stable due to chemisorption (rather than physisorption) and crosslinking caused by EDC.

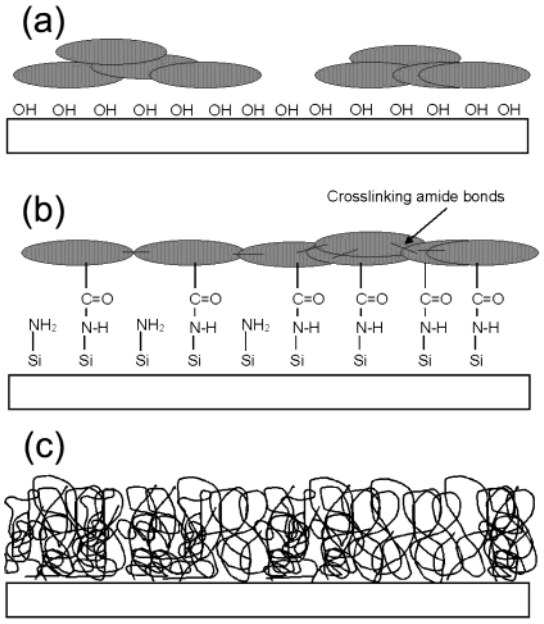

Figure 1. Schematic of (a) protein adsorption on a bare glass surface, (b) protein coupling via amide bonds to an aminosilane-functionalized glass surface using EDC, and (c) PEG binding to amino-functionalized glass.

Surface Topography and Homogeneity. AFM images of BSA physisorbed onto bare glass and chemisorbed onto amino-functionalized glass, crosslinked by EDC, are shown in Figures 2a and b, respectively. Figure 3 shows the corresponding images for streptavidin. From the scale bar on the right of the images, we see an order of magnitude decrease in surface roughness if we chemically bind BSA to the surface, as well as a significant improvement in homogeneity for the streptavidin surface upon chemisorption/crosslinking. Streptavidin is essentially uncharged at neutral pH; therefore, it is expected to adsorb to bare glass less rapidly than BSA, which has a pI of 4.7 and is thus negatively charged at pH 7. Bernabeu and Caprani[42] observed that negatively charged proteins attached strongly to an electrochemically controlled negatively charged surface. This was explained by coadsorption of buffer cations at the surface to render the surface attractive for the protein. Comparison of Figures 2a and 3a yields a similar result, although we do not control the surface charge specifically. The surface of hydrophilic glass consists of silanol groups, which bind water

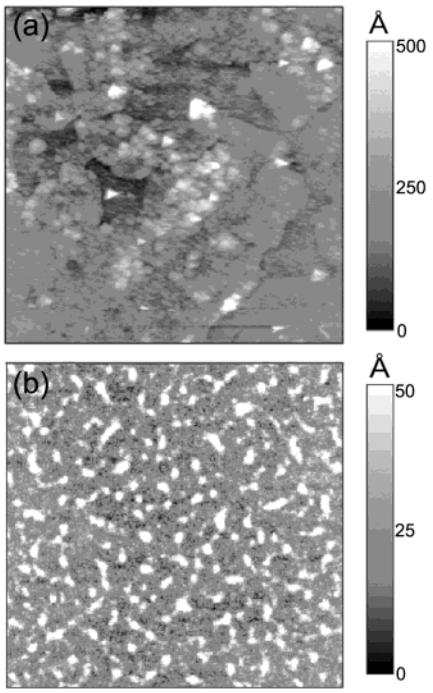

Figure 2. AFM images of (a) BSA physisorbed on a bare glass surface and (b) crosslinked BSA bound to an amino-functionalized surface. Images are 8 μm × 8 μm.

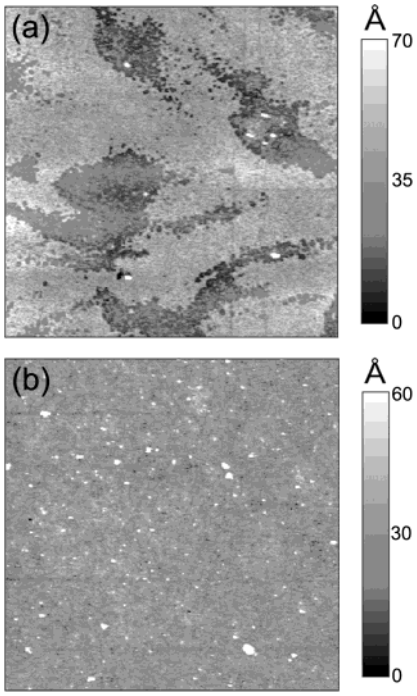

Figure 3. AFM images of (a) streptavidin physisorbed on a bare glass surface and (b) crosslinked streptavidin bound to an amino-functionalized surface. Images are 8 μm × 8 μm.

molecules and can become charged or protonated. Consequently, they adsorb charged particles, such as buffer cations and negative BSA, whereas neutral streptavidin is not so strongly attracted to the glass. This results in the patchy pattern observed in Figure 3a. The difference in height between the patchy layers is approximately 30 Å (about the size of a streptavidin molecule), and points to the possibility of areas of zero coverage and areas of protein monolayer coverage of streptavidin, in stark contrast to the rough multilayer BSA physisorbed surfaces (Figure 2a).

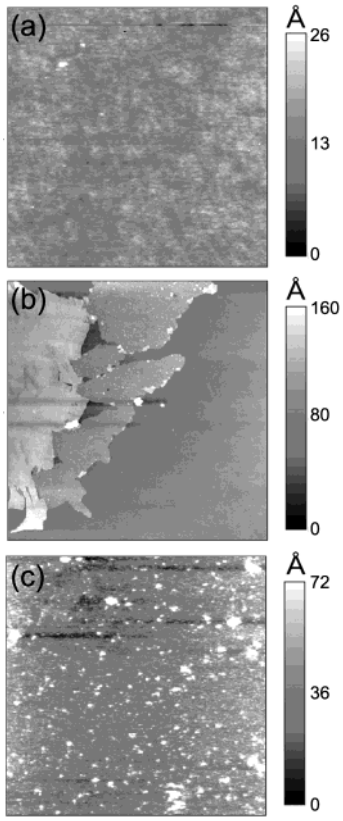

Figure 4. AFM images of linear PEGs bound via an NHS group to amino-functionalized glass surfaces. (a) PEG 5000 at 100 mg/mL solution concentration, (b) PEG 2000 at 100 mg/mL, and (c) PEG 2000 at 1000 mg/mL. Images are 8 μm × 8 μm.

For further comparison of surface heterogeneity, Figure 4 shows AFM images of surfaces covered by chemically linked, linear PEG molecules (MW 5000 or 2000). We see that the PEG-5000-coated surface in Figure 4a is extremely smooth compared with PEG 2000 surfaces made with different polymer concentrations (Figure 4b and c) and protein surfaces. This smoothness has been observed previously.[43] The PEG 2000 surface in Figure 4b is structured on the micrometer scale. It consists of areas of very smooth islands and very smooth valleys with a large step between them. This result was observed repeatedly upon preparation of the films at 100 mg/mL (10% w/v) PEG 2000 concentration, but was not observed at 1000 mg/mL (100% w/v) (Figure 4c). This result can be explained in terms of the relationship between molecular weight, grafting density, and PEG monolayer structure.

Sofia et al.[24] studied experimentally and theoretically the grafting density as a function of molecular weight. They derived the grafting density of linear PEG chains, σ, as

$$\sigma = \frac{\rho_{\mathrm{dry}} h N_A a^2}{M}$$

where ρ_{dry} is the density of the dry PEG layer (typically 1 g/mL), h is the PEG layer thickness, N_A is Avogadro's number, a is the size of the monomer unit (~3 Å), and M is the molecular weight of the PEG chain.

Yang et al.[43] measured the roughness of PEG 5000 and PEG 750 monolayers. The smoother PEG 5000 films were considered the result of a mushroomlike architecture, in which the long chains graft at lower density, intermingle, and flatten out at the surface. PEG 750, on the other hand, is grafted at high density and forms a brush-like architecture with larger average height,

slightly rougher at the surface. The grafting density was measured by Sofia et al. for PEGs with different molecular weights.[24] For 10% w/v solution concentrations (as used in our experiments), a plateau (saturation) was reached in grafting density for all PEG layers, which increased with decreasing PEG molecular weight. Thus, PEG 5000 grafts at relatively low densities and forms mushroomlike surfaces, while PEG 750 grafts at high densities and forms brushlike architectures.[43] The critical concentration marking the overlap of PEG chains in solution is given in Sofia et al.[24] as

$$C_{\mathrm{crit}} = \left(\frac{M}{N_A {}^4/_3 \pi R_{\mathrm{G}}{}^3}\right)$$

where R_G is the radius of gyration of the PEG chain; it is calculated by Devanand et al. as[44]

$$R_{\mathrm{G}} = 0.215 M^{0.583}$$

Thus, for PEG 5000, $R_G = 30$ Å, and the critical concentration is calculated to be ~6.5% (w/v). For PEG 2000, $R_G = 18$ Å and the critical concentration is ~13%. Therefore, at 10% (w/v) concentration, PEG 5000 molecules overlap in solution, whereas PEG 2000 polymer chains predominantly exist as noninteracting, free molecules; only a small fraction of these overlap. This results in completely homogeneous coverage of the surface with PEG5000 in a mushroomlike architecture. PEG 2000, which generally grafts to the surface at higher density, will show areas of brush-like architecture and areas of lower density, mushroomlike structure. Each type of architecture is relatively smooth in itself, but the difference in layer thickness can be large, as seen in Figure 4b. In the brushlike and mushroomlike structures, the film thicknesses were ~85% and ~25% of the chain length, respectively.[43] For brushlike PEG 2000 (~45 ethylene glycol units of ~3 Å each), this thickness corresponds to 0.85 × (3 Å × 45) = 115 Å, and for mushroomlike PEG 2000, the thickness is 0.25 × (3 Å × 45) = 35 Å. The difference of 80 Å is very close to the step height difference observed in Figure 4b, supporting our view that both types of architectures exist on PEG 2000 surfaces. At higher concentrations, PEG 2000 forms only brushlike layers due to the maximal grafting density. These appear as the more homogeneous films in Figure 4c. However, these are still not as smooth as the ones formed by PEG 5000, due to the less homogeneous brushlike structure, as has been previously observed for PEG 750.[43] The type of PEG layer architecture is important, since these have effects on nonspecific protein adsorption properties, as will be discussed below.

The results of the surface homogeneity measurements are summarized in Figure 5. For each of the surfaces, the root-mean-square (RMS) roughness values were calculated for several images (of the same and different samples) to assess this parameter and sample-to-sample variations. The average roughness, together with the standard deviation, is displayed for each surface. Both of these parameters are extremely important in determining the best-suitable surface for single-molecule experiments. Bare glass has a very low RMA roughness, as does Vectabond (aminosilane) functionalized glass. Images of these show very flat and smooth, featureless surfaces (not shown), similar to those of PEG 5000 (Figure 4a). We would expect this to vary significantly with the source and quality of the glass slides, but the slides purchased from Menzel, which were used in these studies, always showed this exceptional smoothness at 8-μm length scales. In general, proteins physisorbed on bare glass substrates display high roughness and

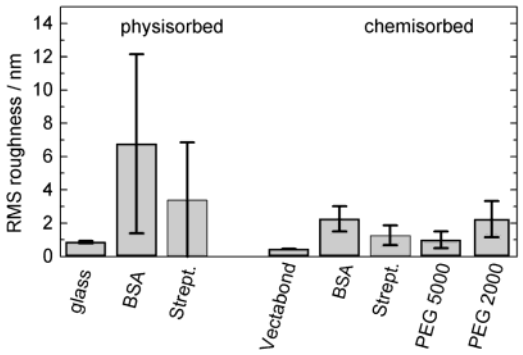

Figure 5. Root-mean-square (RMS) roughness of proteins (BSA and streptavidin) and polymers (PEG 5000 and PEG 2000) physisorbed onto untreated glass and chemisorbed onto amino-functionalized glass surfaces. The data were extracted from several AFM images of each surface; standard deviations are indicated.

large fluctuations in reproducibility. The physisorbed streptavidin layer is smoother than the physisorbed BSA layer, even though there are areas of lower coverage in the streptavidin layer (Figures 2a and 3a). Chemical binding and crosslinking of the proteins on the surface increases the homogeneity substantially, with the streptavidin surface again being smoother than the BSA surface. We suggest that the relatively slow crosslinking process using EDC, together with the slower surface adsorption process of streptavidin due to its neutral pI, allows the system to be thermodynamically guided to its lowest free energy state, yielding a smooth layer. In contrast, rapid absorption (physisorption on bare glass) is kinetically controlled, which leads to a rough layer. Again, this process depends on the net charge of the adsorbed proteins, which most likely explains the differences observed in physisorbed BSA and streptavidin. Furthermore, this kinetic control leads to rather irreproducible layers, varying from 1 to 12 nm in RMS roughness.

It must be noted at this point that the AFM measurements were performed in air, and not under water. During the sample preparation, however, the water was simply allowed to slowly evaporate, it was not forcibly dried, and the measurements were taken within an hour of evaporation in a humid atmosphere. The native protein structure can change upon drying, and this may affect these results, but the relatively mild drying conditions employed should not cause significant changes compared to the protein layer under water. The quantitative RMS roughness may be slightly different under water, but the qualitative behavior of smaller RMS roughness and increased reproducibility upon chemisorption and crosslinking of proteins should not change.

This variation in film thickness indicates that a biomolecule experiences very different environmental conditions at the surface that may affect each molecule's energetics. This is a huge problem in single-molecule studies, which aim to characterize intrinsic heterogeneous behavior rather than uncontrolled external variations. Chemisorption of BSA or streptavidin (together with crosslinking) on amino-functionalized surfaces not only leads to a smoother surface, but also results in better reproducibility of the layer. Therefore, we expect less surface-induced heterogeneity in single molecule experiments.

Resistance to Nonspecific Adsorption of Proteins. Besides homogeneity of the surfaces, minimal interaction is required between the surface and the biomolecule of interest. This important criterion can be addressed through the resistance of the surface to nonspecific adsorption. For this characterization, we have used a small enzyme, RNase H, labeled with biotin and a single dye molecule. The RNase H solution was exposed to our different biotinylated surfaces. For specific binding,

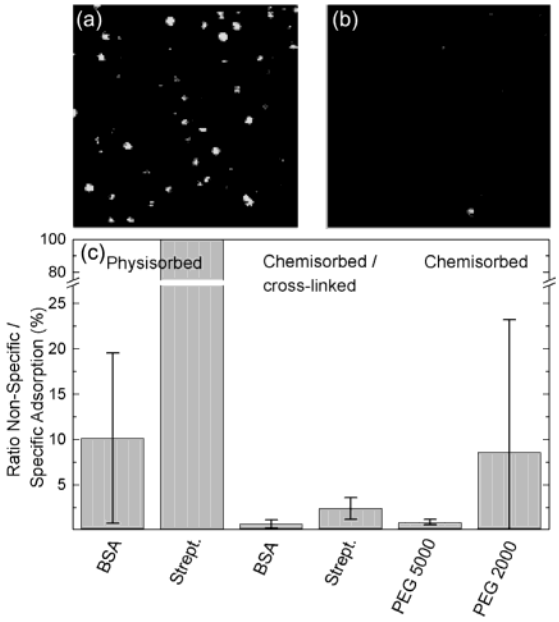

Figure 6. Fluorescence microscopy images (18 μm × 18 μm) of (a) specifically bound RNase H by biotin/streptavidin coupling and (b) RNase H bound nonspecifically to chemisorbed/crosslinked BSA surfaces. (c) Ratio of nonspecific to specific adsorption for each surface, with standard deviations obtained from sample-to-sample variations.

streptavidin was first bound to the surface (Figure 6a), and for nonspecific binding (Figure 6b), streptavidin was omitted. For the streptavidin surfaces, a nonbiotinylated RNase H was used for nonspecific adsorption as described in the Experimental Section. Fluorescence microscopy images were taken to measure the densities of spots from individual RNase H molecules. The ratio of nonspecific to specific adsorption was calculated as a quality measure for each surface (Figure 6c). Large surface areas (typically 20 images of 18 × 18 μm^2 are used for each sample) and multiple samples were measured to increase the statistical significance of these measurements. Both average values and standard deviations were calculated to assess the reproducibility of the protein resistance. Note that we define resistance to nonspecific binding as the ratio of proteins that stick to the surface by means other than the biotin/streptavidin coupling during the incubation period (10 min) compared to the ones that do, and not by the long-term protein deposition on the surface, as is often reported in the biomedical and biomaterials communities. We use our definition of adsorption resistance because we demand that the proteins are immobilized by the same linkage on a homogeneous, biocompatible surface, which minimizes heterogeneities in measurements due to surface artifacts. However, there is no reason that this type of ultrasensitive single-molecule fluorescence method cannot be used for the determination of long-term protein resistance of surfaces in biomedical and biomaterials applications. In fact, we believe that many advantages are to be gained from doing so.

Figure 6c shows that the chemisorbed/crosslinked protein (BSA or streptavidin) surfaces exhibit excellent resistance to nonspecific binding, with ratios of less than 5%. Moreover, they are very reproducible from sample to sample. By contrast, surfaces coated with physisorbed proteins are much less effective. In particular, we found that physisorbed streptavidin does not prevent unspecific adsorption at all. This is most likely due to the low adsorption of the charge-neutral streptavidin on the bare glass, as evidenced from the large patchy areas of uncovered surface for physisorbed streptavidin in the AFM images (Figure 3a). Even after overnight incubation, complete coverage was not achieved, as judged from the poor resistance to protein adsorption (results not shown). Physisorbed BSA is less disposed to nonspecific adsorption than streptavidin, but the error bars represent large sample-to-sample variations. Crosslinking with EDC improves both resistance and reproducibility of nonspecific adsorption for both proteins, yielding homogeneous surface architectures with complete protein coverage (Figure 5). The similar inertness of both chemisorbed/crosslinked BSA and streptavidin suggest that charges on the protein have little or no effect once the protein layer is formed. However, published pI values are measured in solution and not when adsorbed on the surface. Most likely, the pI changes considerably when adsorbed on the surface, due to partial or complete denaturation. Moreover, preferential interaction of particular patches on the protein with the surface can also change the accessibility of charges from the solvent. That said, the chemisorbed streptavidin surface still binds biotin, so a fraction of proteins are still properly folded and functional, at least for one of the four biotin-binding sites.

For the PEG-coated surfaces, Figure 6c shows that PEG 5000 is more resistant to nonspecific binding than PEG 2000. Moreover, the results are much less reproducible with PEG 2000. As shown above, PEG 2000 and PEG 5000 have very different surface properties in terms of homogeneity and grafting architecture (Figure 4b). The larger PEG 5000 most likely exists on the surface in mushroomlike configuration only, with complete overlap of neighboring chains. However, the smaller PEG 2000 exists in both mushroomlike and brushlike structures when grafted at 10% (w/v) concentrations, and is completely brushlike at higher concentrations. The resistance to protein adsorption has been proposed to be very different for these two structure types,[23,25,45] especially for small proteins. There is much less entropy loss for proteins adsorbing to the glass surface between brushes than to mushroomlike surfaces, where they have to expel solvation water molecules before contacting the surface. For this reason, nonspecific adsorption of the small RNase H enzyme on PEG 5000 is much lower than on PEG 2000 with its mixture of the two conformations. Increasing or decreasing the grafting concentration of PEG 2000 does not have an effect (results not shown) for several reasons. At high grafting concentrations, only brushlike PEG 2000 is formed, which is not very efficient at preventing nonspecific adsorption of small proteins (as discussed above). At intermediate concentrations around 10% (w/v), mixtures of the two architectures coexist. The mushroomlike regions would be adsorption resistant, but the brushlike regions would not be adsorption resistant. Thus, adsorption to the brushlike regions yields overall low nonspecific binding resistance. At very low concentrations, there are large areas of the glass not covered by PEG 2000, resulting in low resistance. This discussion will not hold true if the protein diameter is much larger than the space between brushes,[25] in which case higher grafting density should yield higher resistance. The dependence of protein diameter on surface adsorption was observed experimentally by Sofia et al.[24] using higher-molecular-weight PEGs.

Protein Structure on Biocompatible Surfaces. From the above measurements, it would seem as though PEG-5000-coated surfaces are an excellent choice for single-biomolecule experiments, since they resist nonspecific adsorption and form homogeneously smooth layers. However, we also require that specifically bound proteins should maintain their properly folded, native conformations. To examine if RNase H enzyme molecules retain their native folds upon surface immobilization, we performed FRET measurements with PEG 5000, physisorbed

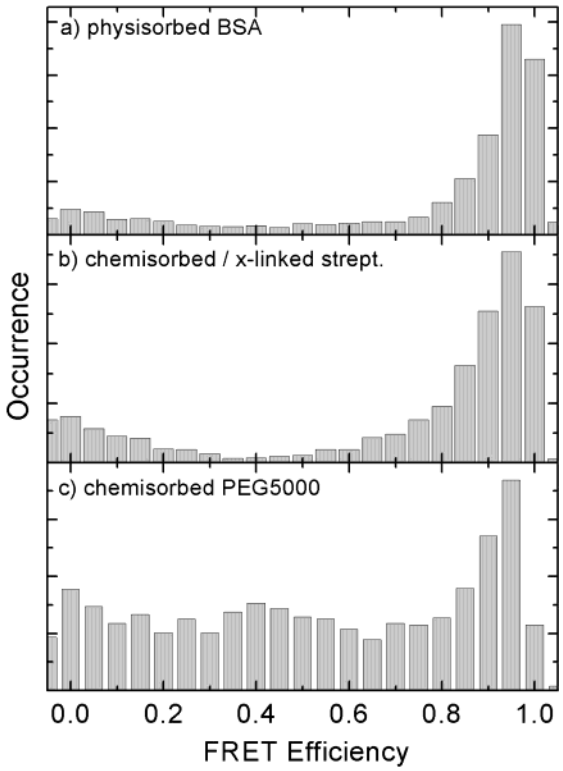

Figure 7. FRET efficiency histograms of RNase H on (a) physisorbed BSA, (b) chemisorbed/crosslinked streptavidin, and (c) PEG 5000 surfaces. Complete FRET efficiency is observed on the protein surfaces, whereas a distribution of efficiencies is observed on PEG 5000. This highlights the interacting nature of PEG surfaces with RNase H.

BSA, and chemisorbed and crosslinked streptavidin surfaces. Two dye attachment sites were engineered into the protein to ensure that the dyes are in close proximity when the protein is properly folded, and relatively far apart when unfolded. For each individual molecule on the surface, the efficiency of energy transfer, η, was calculated from the photon counts in the red channel, $I_{A,}$ and green channel, I_D, as

$$\eta = \frac{I_A}{I_A + \gamma I_D}$$

Here, γ is a correction factor that accounts for the different detection efficiencies in the two channels. The FRET efficiency depends strongly, that is, to the sixth power, on the distance between the two dye molecules. Therefore, in the compact, folded state, excitation of the green dye results in essentially complete energy transfer ($\eta \approx 1$) to the red acceptor dye. In the unfolded, denatured conformation, the FRET efficiency will be less. In Figure 7, we plot the FRET efficiencies for a large number of RNase H molecules. For the BSA and streptavidin surfaces, we observe a large distribution close to $\eta = 1$, indicating that the predominant fraction of enzymes indeed retain their folded states. A second maximum near zero FRET efficiency arises from protein molecules that have either lost their red acceptor dye due to photobleaching or dissociation, or from the situation where there was no red dye attached during labeling, as has been observed previously.[1] By contrast, PEG 5000 surfaces exhibit a broad, featureless distribution of FRET efficiencies. The peak near $\eta \approx 1$ is less pronounced, and all other FRET efficiencies have an almost equally likely occurance. Consequently, only small fractions of molecules are still in their native conformations. The wide variation of interdye distances for the majority of the molecules represents a broad distribution of conformations. Apparently, the PEG 5000 surface causes unfolding of the RNase. We suggest that the highly flexible, long PEG chains penetrate into the protein interior, where they replace intra-protein interactions. A similar effect of PEG was observed by Lee and Lee,[46] who reported a decreased thermal stability of proteins in PEG solutions. In this study, hydrophobic proteins were shown to be most sensitive to the presence of PEG, whereas RNase A, being relatively hydrophilic, was largely unaffected (RNase H has a similar surface hydrophilicity as RNase A and thus should behave similarly.). Little destabilization was observed in solution for most proteins with high-molecular-weight PEG 4000. It was concluded that, in solution, PEG chains interact preferentially with hydrophobic regions and avoid charged residues, such as the ones on the surface of RNase A. Moreover, for long PEG chains, it will be more difficult to only interact with hydrophobic regions while simultaneously avoiding hydrophilic ones. Immobilized on surfaces, however, the PEG chains and proteins are forced into close proximity. The PEG chains may interact with hydrophobic, internal residues of the protein, whenever a protein molecule performs a rare thermal fluctuation that exposes these sites. In the end, this will lead to intermingling of the PEG and polypeptide chains, thus stabilizing a non-native state of the protein. In our case, this only happens when they are immobilized together on the surface. When the surface-immobilized RNase H (not immobilized on PEG surfaces) is placed in a high concentration PEG solution (50% w/v), such as is used during the RNase H purification,[38,39] no such denaturation was evident (results not shown), and the FRET distribution shows only a single peak at $\eta \approx 1$, supporting our view that it is the surface-immobilized PEG stabilizing the unfolded state One other possibility for chain intermingling of PEG and protein is that the folded protein can eventually penetrate the flexible PEG layer and become strongly bound to the underlying aminosilane layer, which in turn stabilizes the unfolded state. This possibility arises due to the low grafting density of large PEG chains to the surface. In contrast, the physisorbed or chemisorbed protein surfaces are much less flexible than PEG and cannot have such a destabilizing effect on proteins immobilized on them. Crosslinked protein layers do not have extended chains at all and are thus even better for preparing surfaces for immobilization of single molecules than physisorbed proteins, linear PEG 5000 chains, or linear PEG 2000 chains. Thus, though linear PEGs are widely regarded as promising biomedical materials, RNase H is destabilized when immobilized on PEG 5000 surfaces. This may be a general property of small proteins on PEG surfaces, but further experiments are needed to make this determination.

Conclusions

Single-molecule fluorescence microscopy studies with immobilized protein molecules require homogeneous, minimally interacting, and adsorption-resistant surfaces on glass or quartz substrates. By using AFM and single-molecule fluorescence-microscopy techniques, we have systematically characterized various biocompatible, biotinylated surfaces for their usefulness as ultrathin coatings, on which the proteins under study can be immobilized by streptavidin−biotin conjugation. We have compared physisorbed protein, chemisorbed/crosslinked protein, and chemisorbed PEG layers with respect to surface homogeneity, resistance to nonspecific binding, and preservation of the native fold of the immobilized protein, for which we took RNase H as an example. Chemisorbed, crosslinked protein layers yielded much more homogeneous and very reproducible surfaces than physisorption, with less than 5% nonspecific adsorption. Moreover, FRET experiments showed that specifically bound

RNase H molecules retain their native folds on these layers. Similar to the crosslinked protein layers, PEG 5000 provides homogeneously smooth surfaces and high resistance to nonspecific binding, whereas PEG 2000 is both less homogeneous and less resistant. We attribute this to differences in surface architecture of PEG 5000 and PEG 2000. PEG 5000, however, causes denaturation of the RNase H structure. This was attributed to the flexible PEG chains interacting with the hydrophobic interior of the protein or to the interaction of the protein with the underlying aminosilane layer, either of which stabilizes unfolded conformations. Therefore, we conclude that protein surfaces are better suited for certain single-molecule experiments than surfaces coated with linear PEG chains. The excellent homogeneity provided by chemisorption/crosslinking of proteins onto amino-functionalized surfaces will promote reproducibility and reduce heterogeneities in single molecules due to surface artifacts. These results show that it is imperative to thoroughly characterize surfaces that are to be used for single molecule experiments.

Acknowledgment. C.D.H would like to thank the Alexander von Humboldt Foundation and the Human Frontiers Science Program for research fellowships. We thank Sigrid Niederhausen-Kraft for help in the preparation of the functionalized surfaces, Uwe Theilen for help in the growth and purification of the RNase H, and Prof. Dr. Othmar Marti for his expert assistance with the AFM. Financial support from the Deutsche Forschungsgemeinschaft (SFB569), 'Fonds der Chemischen Industrie' and the 'Landesforschungs-schwerpunktprogramm Baden-Württemberg' is gratefully acknowledged.

References and Notes

(1) Schuler, B.; Lipman, E. A.; Eaton, W. A. *Nature* **2002**, *419*, 743−747.

(2) Rhoades, E.; Gussakovsky, E.; Haran, G. *Proc. Natl. Acad. Sci. U.S.A.* **2003**, *100*, 3197−3202.

(3) Deniz, A. A.; Laurence, T. A.; Beligere, G. S.; Dahan, M.; Martin, A. B.; Chemla, D. S.; Dawson, P. E.; Schultz, P. G.; Weiss, S. *Proc. Natl. Acad. Sci. U.S.A.* **2000**, *97*, 5179−5184.

(4) Kim, H. D.; Nienhaus, G. U.; Ha, T.; Orr, J. W.; Williamson, J. R.; Chu, S. *Proc. Natl. Acad. Sci. U.S.A.* **2002**, *99*, 4284−4289.

(5) Dickson, R. M.; Cubitt, A. B.; Tsien, R. Y.; Moerner, W. E. *Nature* **1997**, *388*, 3558−3358.

(6) Wiedenmann, J.; Schenk, A.; Rocker, C.; Girod, A.; Spindler, K. D.; Nienhaus, G. U. *Proc. Natl. Acad. Sci. U.S.A.* **2002**, *99*, 11646−11651.

(7) Borsch, M.; Diez, M.; Zimmermann, B.; Reuter, R.; Graber, P. *FEBS Lett.* **2002**, *527*, 147−152.

(8) Ha, T.; Ting, A. Y.; Liang, J.; Caldwell, W. B.; Deniz, A. A.; Chemla, D. S.; Schultz, P. G.; Weiss, S. *Proc. Natl. Acad. Sci. U.S.A.* **1999**, *96*, 893−898.

(9) Eigen, M.; Rigler, R. *Proc. Natl. Acad. Sci. U.S.A.* **1994**, *91*, 5740−5747.

(10) Deniz, A. A.; Dahan, M.; Grunwell, J. R.; Ha, T.; Faulhaber, A. E.; Chemla, D. S.; Weiss, S.; Schultz, P. G. *Proc. Natl. Acad. Sci. U.S.A.* **1999**, *96*, 3670−3675.

(11) Weiss, S. *Nat. Struct. Biol.* **2000**, *7*, 724−729.

(12) Lamb, D. C.; Schenk, A.; Rocker, C.; Scalfi-Happ, C.; Nienhaus, G. U. *Biophys. J.* **2000**, *79*, 1129−1138.

(13) Zemanova, L.; Schenk, A.; Valler, M. J.; Nienhaus, G. U.; Heilker, R. *Drug Discovery Today* **2003**, *in press*.

(14) Talaga, D. S.; Lau, W. L.; Roder, H.; Tang, J.; Jia, Y.; DeGrado, W. F.; Hochstrasser, R. M. *Proc. Natl. Acad. Sci. U.S.A.* **2000**, *97*, 13021−13026.

(15) Boukobza, E.; Sonnenfeld, A.; Haran, G. *J. Phys. Chem. B* **2001**, *105*, 12165−12170.

(16) Kingshott, P.; Griesser, H. J. *Curr. Opin. Sol. State Mater. Sci.* **1999**, *4*, 403−412.

(17) Ostuni, E.; Chapman, R. G.; Holmlin, R. E.; Takayama, S.; Whitesides, G. M. *Langmuir* **2001**, *17*, 5605−5620.

(18) Ulman, A. *Chem. Rev.* **1996**, *96*, 1533−1554.

(19) Mrksich, M.; Whitesides, G. M. *Annu. Rev. Biophys. Biomol. Struct.* **1996**, *25*, 55−78.

(20) Harris, J. M.; Zalipsky, S. *Poly(ethylene glycol): Chemistry and Biological applications*; American Chemical Society: Washington DC, 1997.

(21) Prime, K. L.; Whitesides, G. M. *J. Am. Chem. Soc.* **1993**, *115*, 10714−10721.

(22) Szleifer, I. *Biophys. J.* **1997**, *72*, 595−612.

(23) Satulovsky, J.; Carignano, M. A.; Szleifer, I. *Proc. Natl. Acad. Sci. U.S.A.* **2000**, *97*, 9037−9041.

(24) Sofia, S. J.; Premnath, V.; Merrill, E. W. *Macromolecules* **1998**, *31*, 5059−5070.

(25) Halperin, A. *Langmuir* **1999**, *15*, 2525−2533.

(26) Zolk, M.; Eisert, F.; Pipper, J.; Herrwerth, S.; Eck, W.; Buck, M.; Grunze, M. *Langmuir* **2000**, *16*, 5849−5852.

(27) Harder, P.; Grunze, M.; Dahint, R.; Whitesides, G. M.; Laibinis, P. E. *J. Phys. Chem. B* **1998**, *102*, 426−436.

(28) Feldman, K.; Hähner, G.; Spencer, N. D.; Harder, P.; Grunze, M. *J. Am. Chem. Soc.* **1999**, *121*, 10134−10141.

(29) Sackmann, E. *Science* **1996**, *271*, 43−48.

(30) Ross, E. E.; Spratt, T.; Liu, S.; Rozanski, L. J.; O'Brien, D. F.; Saavedra, S. S. *Langmuir* **2003**, *19*, 1766−1774.

(31) Trabesinger, W.; Schütz, G. J.; Gruber, H. J.; Schindler, H.; Schmidt, T. *Anal. Chem.* **1999**, *71*, 279−283.

(32) Forkey, J. N.; Quinlan, M. E.; Shaw, M. A.; Corrie, J. E. T.; Goldman, Y. E. *Nature* **2003**, *422*, 399−404.

(33) Massia, S. P.; Stark, J.; Letbetter, D. S. *Biomaterials* **2000**, *21*, 2253−2261.

(34) Delgado, A. D. S.; Léonard, M.; Dellacherie, E. *Langmuir* **2001**, *17*, 4386-4391.

(35) Mrksich, M. *Chem. Soc. Rev.* **2000**, *29*, 267−273.

(36) Sakamoto, T.; Amitani, I.; Yokota, E.; Ando, T. *Biochem. Biophys. Res. Commun.* **2000**, *272*, 586−590.

(37) Piestert, O.; Barsch, H.; Buschmann, V.; Heinlein, T.; Knemeyer, J.-P.; Weston, K. D.; Sauer, M. *Nano Lett.* **2003**, *3*, 979−982.

(38) Kanaya, S.; Crouch, R. *J. Biol. Chem.* **1983**, *258*, 1276−1281.

(39) Kanaya, S.; Kohara, A.; Miyagawa, M.; Matsuzaki, T.; Morikawa, K.; Ikehara, M. *J. Biol. Chem.* **1989**, *264*, 11546−11549.

(40) Hermanson, G. T. *Bioconjugate Techniques*; Academic Press: San Diego, 1996.

(41) Ramsden, J. J. *Chem. Soc. Rev.* **1995**, *24*, 73−79.

(42) Bernabeu, P.; Caprani, A. *Biomaterials* **1990**, *11*, 258−264.

(43) Yang, Z.; Galloway, J. A.; Yu, H. *Langmuir* **1999**, *15*, 8405−8411.

(44) Devanand, K.; Selser, J. C. *Macromolecules* **1991**, *24*, 5943−5947.

(45) Szleifer, I.; Carignano, M. A. *Macromol. Rapid. Commun.* **2000**, *21*, 423−448.

(46) Lee, L. L. Y.; Lee, J. C. *Biochemistry* **1987**, *26*, 7813−7819.